IEEE Photonics Journal
An IEEE Photonics Society Publication

Open Access

AquaE-lite Hybrid-Solar-Cell Receiver-Modality for Energy-Autonomous Terrestrial and Underwater Internet-of-Things

Volume 12, Number 4, 2020

Meiwei Kong
Jiaming Lin
Yujian Guo
Xiaobin Sun
Mohammed Sait
Omar Alkhazragi
Chun Hong Kang
Jorge A. Holguin-Lerma
Malika Kheireddine
Mustapha Ouhssain
Burton H. Jones
Tien Khee Ng
Boon S. Ooi

DOI: 10.1109/JPHOT.2020.3013995

IEEE photonics SOCIETY
IEEE

AquaE-lite Hybrid-Solar-Cell Receiver-Modality for Energy-Autonomous Terrestrial and Underwater Internet-of-Things

Meiwei Kong [1], Jiaming Lin [2], Yujian Guo [1], Xiaobin Sun [1], Mohammed Sait,[1] Omar Alkhazragi [1], Chun Hong Kang [1], Jorge A. Holguin-Lerma [1], Malika Kheireddine,[3] Mustapha Ouhssain,[3] Burton H. Jones [3], Tien Khee Ng [1], and Boon S. Ooi [1]

[1]Photonics Laboratory, King Abdullah University of Science and Technology (KAUST), Thuwal 23955-6900, Saudi Arabia
[2]Optical Communications Laboratory, Ocean College, Zhejiang University, Zhoushan 316021, China
[3]Integrated Ocean Processes Laboratory, King Abdullah University of Science and Technology (KAUST), Thuwal 23955-6900, Saudi Arabia

DOI:10.1109/JPHOT.2020.3013995

Manuscript received June 17, 2020; revised July 23, 2020; accepted July 30, 2020. Date of publication August 4, 2020; date of current version August 18, 2020. This work was supported by the King Abdullah University of Science and Technology (KAUST) under Grants BAS/1/1614-01-01, KCR/1/2081-01-01, KCR/1/4114-01-01, and GEN/1/6607-01-01. (Meiwei Kong and Jiaming Lin contributed equally to this work) Corresponding author: Boon S. Ooi (e-mail: boon.ooi@kaust.edu.sa).

Abstract: Our goal is to develop an energy-autonomous solar cell receiver that can be integrated with a variety of smart devices to implement the Internet of Things in next-generation applications. This paper details efforts to develop such a prototype, called AquaE-lite. Owing to the capability of detecting low-intensity optical signals, 20-m and 30-m long-distance lighting and optical wireless communication with data rates of 1.6 Mbit/s and 1.2 Mbit/s have been achieved on a laboratory testbed, respectively. Moreover, field trials on an outdoor solar cell testbed and in the turbid water of a harbor by the Red Sea have been conducted. Under bright sunlight, energy autonomy and 1.2-Mbit/s optical wireless communication over a transmission distance of 15 m have been implemented, which demonstrated that AquaE-lite with an elaborate receiver circuit has excellent performance in energy harvesting and resistance to background noise. In a more challenging underwater environment, 1.2-Mbit/s signals were successfully received over a transmission distance of 2 m. It indicates that energy-autonomous AquaE-lite with large detection area has promising prospects in future underwater mobile sensor networks to significantly relieve the requirement of pointing, acquisition and tracking while resolving the energy issues.

Index Terms: Internet of Things, energy autonomous, solar cell, optical wireless communication.

1. Introduction

The efficient transmission and sharing of power featuring millions of distributed new-energy devices was realized by the Energy Internet in Industry 3.0, owing to developments in information, power electronics, and intelligent management [1]. The remarkable progress of the Energy Internet has

laid a solid foundation for the Energy Internet of Things in Industry 4.0, and will undoubtedly benefit innovations in the upcoming Industry 5.0 standard. With advancements in the industrial revolution, renewable solar energy has been developed to address the global energy crisis and environmental degradation while satisfying people's energy-related demands in daily life. It is well known that photovoltaic (PV) solar cells are the core components for converting solar energy into electricity by using the PV effect. Over the past few years, the development of PV solar cells has rapidly evolved from first-generation silicon (Si) wafer-based solar cells and second-generation thin film-based solar cells to third-generation solar cells based on newly developed light-absorbing materials [2]. The first-generation Si wafer-based solar cells, which feature high stability, high efficiency, and low cost, have been widely deployed in the global solar energy infrastructure [2]. The market penetration of the second-generation thin film-based solar cells has also grown significantly owing to their unique advantages, such as high transparency, flexibility, and light absorption coefficient [3]. With advancements in materials, third-generation solar cells based on new materials (e.g., dye-sensitized, organic, and perovskite-based solar cells) have emerged, and have led to breakthroughs in terms of the photoelectric conversion efficiency (PCE) [4]. However, substantial work is still needed to overcome impediments to the implementation of third-generation solar cells in terms of stability, material growth, and cost of fabrication while accelerating their commercialization in the market.

In recent years, solar cells have shown significant potential for use in optical wireless communication (OWC) [5]–[14]. By converting optical signals into electrical signals by relying on the photoconductive effect without any external power, solar cells are energy-saving and more environmentally friendly than conventional PIN diodes, avalanche photodiodes, and photomultiplier tubes. Moreover, with the addition of external communication circuits, solar cells that are widely used in the solar energy infrastructure and various emerging solar-powered devices (e.g., wearable devices, autonomous vehicles, and unmanned aerial vehicles) can perform the dual functions of energy harvesting and signal detection in OWC. This will facilitate the rapid construction of Internet of Things (IoT) in the future, where data rate of $\sim$ kbit/s or $\sim$ Mbit/s, low power, low cost, high reliability, and large connective density will be in demand [15], [16]. In particular, solar cells that can serve as detectors for simultaneous signal detection and efficient energy harvesting have important application prospects in marine equipment owing to the power shortage in marine environments.

In this paper, a fully energy-autonomous hybrid-solar-cell receiver called AquaE-lite is developed and tested in various application scenarios, where this is the first step toward developing self-powered IoT devices. In this work, we propose and demonstrate the use of a monocrystalline Si solar panel with high PCE for efficient energy harvesting, and a thin-film amorphous Si (a-Si) solar cell with a high light absorption coefficient for low-intensity optical signal detection [5], simultaneously. Compared with the use of only one kind of solar cell for simultaneous energy harvesting and signal detection [5]–[11], the proposed scheme can take full advantage of different types of solar cells to improve the energy harvesting as well as the communication performance of the system. For energy-autonomous IoT devices, we first propose and demonstrate an automatic control scheme that uses a programmable-gain amplifier (PGA). Compared with using an amplifier with a fixed gain, the proposed scheme can automatically adjust gain according to the residual electricity to optimize communication performance. To test communication performance, we conducted an experiment on a laboratory testbed. Using AquaE-lite and a white-light laser, we achieved transmission at distances 20 m and 30 m for illumination and visible light communication (VLC) at data rates of 1.6 Mbit/s and 1.2 Mbit/s, respectively. To study the performance of AquaE-lite in terms of simultaneous energy harvesting and VLC, a field trial was conducted on a PV solar cell testbed located at the King Abdullah University of Science and Technology (KAUST). Energy autonomy was implemented using AquaE-lite under direct sunlight. Moreover, orthogonal frequency-division multiplexing (OFDM) signals at a data rate of 1.2-Mbit/s were obtained over a 15-m air channel. This indicates that AquaE-lite delivers good performance in terms of energy harvesting, low-intensity optical signal detection, and resistance to background noise. We also investigated the communication performance of AquaE-lite in a more challenging underwater environment: namely, in the turbid water of the KAUST harbor by the Red Sea, where a 2-m transmission distance was successfully

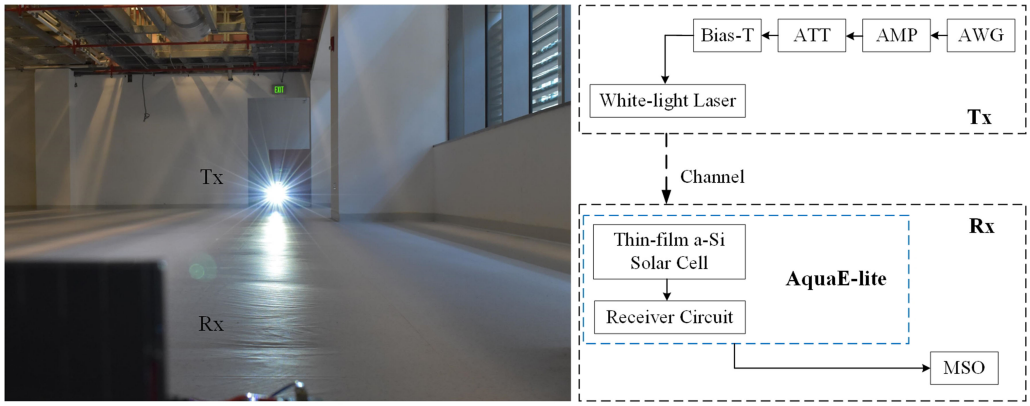

Fig. 1. (a) Experimental scene and (b) schematic diagram of AquaE-lite and white-light laser-based VLC on the laboratory testbed.

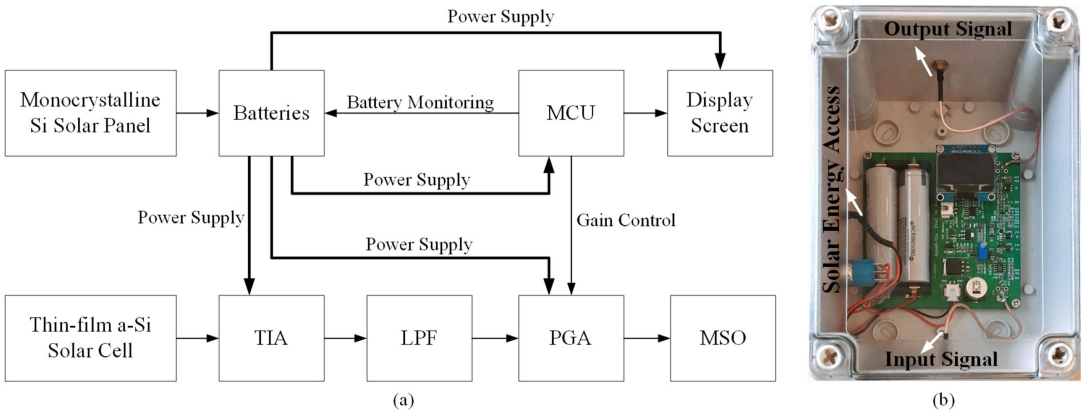

Fig. 2. (a) Schematic diagram of AquaE-lite and (b) photo of the receiver circuit.

implemented without accurate link alignment at a data rate of 1.2 Mbit/s. This indicates that the robust AquaE-lite-based VLC system has significant potential for use in underwater mobile sensor networks to resolve link alignment- and energy-related issues.

2. Experiment on the Laboratory Testbed

2.1 Experimental Setup

Fig. 1(a) shows the experimental scene of AquaE-lite and the white-light laser-based VLC link on the laboratory testbed. Light emitted by indoor fluorescent lights and sunlight entering through windows was the main background noise. A schematic diagram of the VLC system is provided in Fig. 1(b). On the transmitter (Tx) side, four-quadrature amplitude modulation (4-QAM) OFDM signals were first sent by an arbitrary waveform generator (AWG) and then superposed onto the white-light laser by a bias-tee (Bias-T) after being transmitted through an amplifier (AMP) and an attenuator (ATT). The parameters of the devices and OFDM signals have been provided in [5]. White-light laser with a bias current of 670 mA was used for simultaneous illumination and communication. On the receiver (Rx) side, 4-QAM OFDM signals were detected by AquaE-lite. Finally, the output signals were captured by a mixed signal oscilloscope (MSO) and demodulated offline [5].

AquaE-lite consists of an off-the-shelf thin-film a-Si solar cell, a monocrystalline Si solar panel, and a custom-designed receiver circuit. Fig. 2(a) is a schematic diagram of AquaE-lite. A thin-film

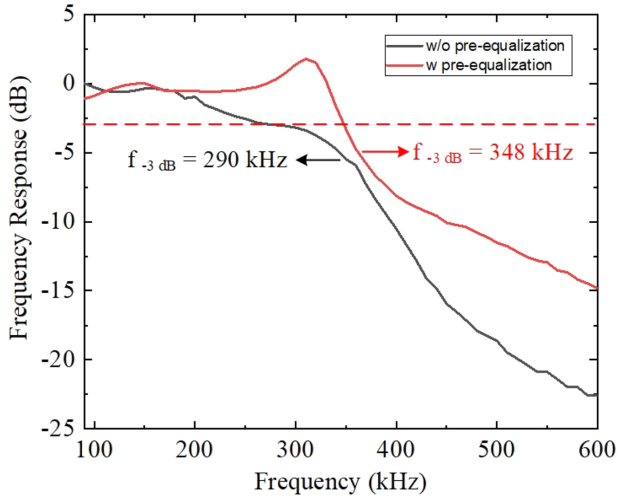

Fig. 3. Frequency response of the AquaE-lite and the white-light laser-based VLC system measured over a 20-m air channel before and after using the hardware equalization.

a-Si solar cell with a length of 6 cm and a width of 6 cm was used for the VLC. It could detect light as weak as 1 μW/cm^2, which is favorable for the implementation of long-distance VLC [5]. To achieve energy balance, the monocrystalline Si solar panel was used for energy harvesting, where two off-the-shelf monocrystalline Si solar cells were connected in series to provide a total active area of 156 cm^2 (length: 13 cm and width: 12 cm). The energy harvested by the monocrystalline Si solar panel was stored in two batteries and used for signal demodulation. When the thin-film a-Si solar cell was used for communication, the generated photocurrent was first converted into voltage by using a trans-impedance amplifier (TIA) and then sent to a low-pass filter (LPF) to remove noise, which improved the signal-to-noise ratio (SNR) of the received signals. Note that a microcontroller unit (MCU) was used to monitor the power of the batteries in real time. The voltage gain of a PGA automatically changes according to the battery power, which can save energy and help enhance communication performance by increasing the amplitudes of the signals. Finally, the output signals were captured by an MSO and demodulated offline. A display screen was used to show the important parameters of AquaE-lite in real time, as shown in Fig. 6. As all the components had consumed a small amount of power, the total consumed electrical power of AquaE-lite was only around 500 mW. Fig. 2(b) presents a photo of the receiver circuit (length: 9 cm, width: 9 cm, and height: 2 cm), which was composed of a display screen, two rechargeable batteries, and a signal-processing circuit. It was packaged in a 17 cm $\times$ 12 cm $\times$ 9 cm white box.

The considerations in developing AquaE-lite are summarized below. They can provide a valuable reference model for the future development of self-powered IoT devices.

- To reduce energy consumption, all components (e.g., TIA, PGA, MCU, and display screen) should be carefully selected, which should have low power consumption.
- Reducing noise to improve communication performance is important. In this work, we used a combination of hardware and software techniques to reduce the noise flexibly. To reduce electrical noise, components with low noise should be selected, which is favorable for the processing of low-intensity signals. Moreover, an LPF can be used to filter out-of-band noise. According to the empirical situation, low-frequency noise can be flexibly removed by using a modulation scheme with appropriate parameters. For example, we employed OFDM and designed empty subcarriers (10 subcarriers) near the DC as a frequency gap to remove low-frequency noise.
- An intelligent power management module is necessary in an energy-autonomous device. When the voltage of the batteries is higher than that of the component to be supplied, a buck converter circuit is required. With the consumption of electricity, a boost converter

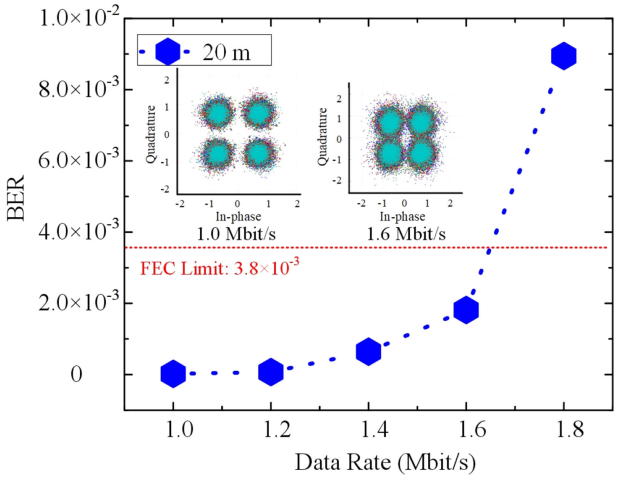

Fig. 4. BER versus data rate over a 20-m air channel while the PGA is at the maximum gain (74 dB). Insets: constellation maps of the 4-QAM OFDM signals at data rates of 1 Mbit/s and 1.6 Mbit/s, respectively.

circuit is required when the voltage of the batteries is lower than that of the component to be supplied. Furthermore, the boost or buck circuit should be designed according to the demands of different components. For example, when supplying power to the display screen, a buck converter circuit is used because it has high power conversion efficiency, despite its high output ripple and switching noise. However, when supplying power to the TIA, a low dropout regulator should be used because it has a low output ripple and switching noise, which enables it to amplify low-intensity signals even though its efficiency of power conversion is lower than that of the buck converter circuit.

- Instead of using an amplifier with a fixed gain, we first demonstrate an automatic control scheme that uses a PGA to optimize the relationship between communication performance and energy use. When the residual power of the batteries is high, the PGA automatically increases the gain, which is favorable for achieving a longer communication distance or a higher data rate. When the residual power of the batteries is low, the PGA automatically reduces the gain to prolong the use time of AquaE-lite.
- Owing to the limited bandwidth of the solar cell, employing a modulation method with high spectral efficiency can improve the data rate, in such terms as pulse amplitude modulation, OFDM, and multiple-input multiple-output schemes.

2.2 Experimental Results

As the experiment on the laboratory testbed was mainly designed to test communication performance rather than charging performance, the thin-film a-Si solar cell was connected to AquaE-lite whereas the monocrystalline Si solar panel was not. The frequency response of the system was first measured over a 20-m air channel. The −3-dB bandwidth of the AquaE-lite and the white-light laser-based VLC system was increased from 290 kHz [5] to 348 kHz by means of hardware pre-equalization, as shown in Fig. 3.

We then studied the maximum data rate that could be achieved over a 20-m air channel while the PGA had its maximum gain (74 dB). The bit error ratio (BER) versus the data rate is illustrated in Fig. 4, where the insets are the constellation maps of the 4-QAM OFDM signals at data rates of 1 Mbit/s and 1.6 Mbit/s, respectively. Note that we recorded symbols sent over different periods and calculated the average BER to improve reliability in the experiment. Therefore, different colors in the constellation maps represent symbols sent over different periods. It shows that the achievable maximum data rate was 1.6 Mbit/s with a BER of 1.814×10^{-3}, below the forward error correction (FEC) limit of 3.8×10^{-3}.

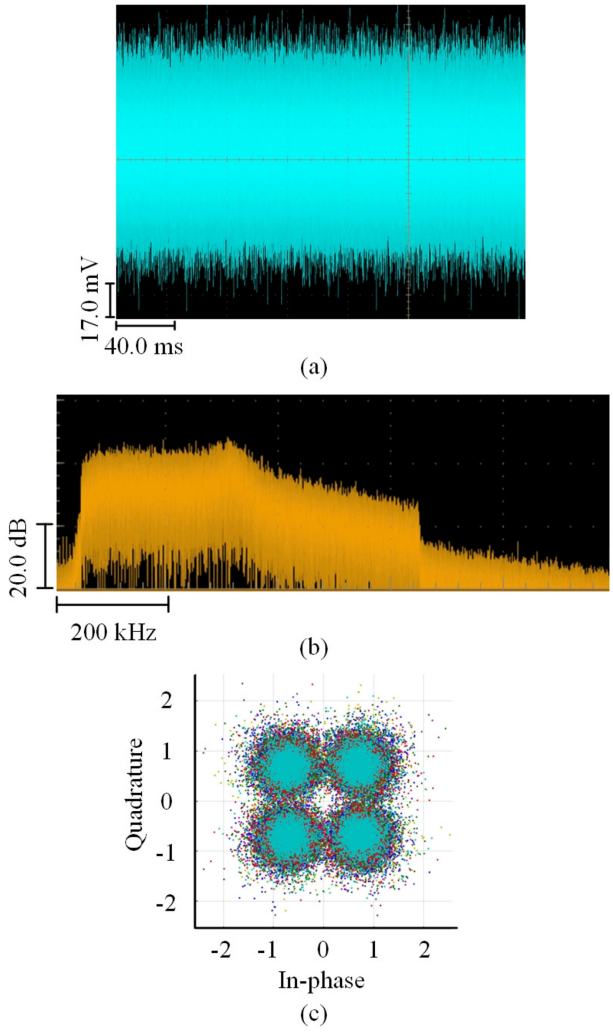

Fig. 5. (a) Waveform, (b) spectrum, and (c) constellation map of the 1.2-Mbit/s OFDM signals at 30 m while the PGA is at the maximum gain (74 dB).

We further investigated the maximum data rate that could be supported by the maximum gain of the PGA (74 dB) at a longer distance of 30 m. The BERs of the 1-Mbit/s, 1.2-Mbit/s, and 1.4-Mbit/s OFDM signals were 2.257×10^{-3}, 2.131×10^{-3}, and 6.450×10^{-3}, respectively. Thus, the maximum data rate at 30 m was 1.2 Mbit/s. The corresponding waveform, spectrum, and constellation map are presented in Figs. 5(a), 5(b), and 5(c), respectively. From the waveform, we see that the mean peak-to-peak amplitude of the 1.2-Mbit/s OFDM signals amplified by the PGA at the receiver side was up to 160.9 mV over the 30-m air channel, which provided a relatively high SNR. The spectrum also demonstrated that the SNR was high enough to support 600-kHz (i.e., 1.2 Mbit/s) signal transmission.

Considering that the gain in the PGA decreased with the consumption of battery energy in the receiving circuit, we studied the effect of PGA gain on communication performance. The gain in the PGA at different battery levels was shown on the display screen (see Fig. 6), where V_{sun} and I_{sun} represent the output voltage and the current of the monocrystalline Si solar panel, respectively. Thus, the product of V_{sun} and I_{sun} is the power harvested from sunlight. As the monocrystalline Si solar panel was not connected to AquaE-lite, V_{sun} and I_{sun} were 0 V and 0 mA, respectively. V_b and I_b represent the total consumed voltage and current of the two batteries, respectively. Power represents the power consumed by AquaE-lite, the product of V_b and I_b. Gain refers to the gain

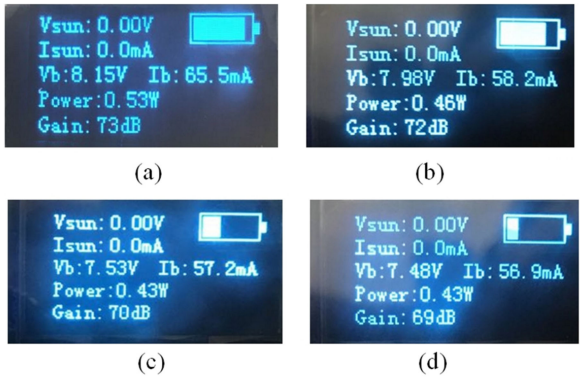

Fig. 6. Photos of the display screen on the receiver circuit of AquaE-lite at the PGA gain of (a) 73 dB, (b) 72 dB, (c) 70 dB, and (d) 69 dB, which show the output voltage (V_{sun}) and the current (I_{sun}) of the monocrystalline Si solar panel for energy harvesting, the total consumed voltage (V_b) and current (I_b) of the two batteries on the receiver circuit of AquaE-lite, the power consumed by the receiver circuit of AquaE-lite (Power), and the PGA gain values (Gain).

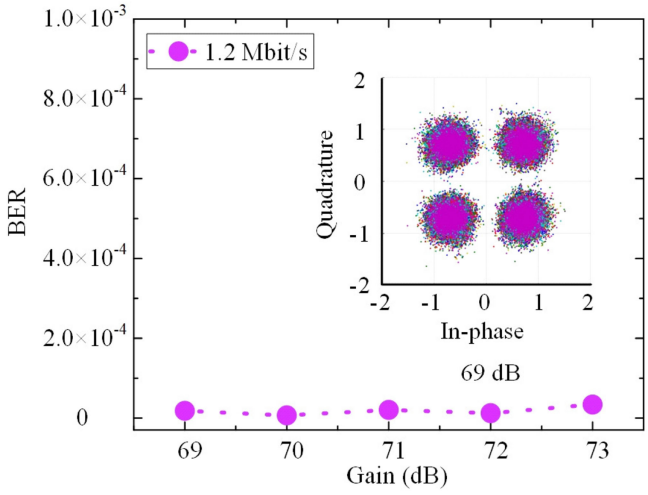

Fig. 7. BERs of the 1.2-Mbit/s 4-QAM OFDM signal as the gain of the PGA decreased from 73 dB to 69 dB. Inset: constellation map of the 1.2-Mbit/s 4-QAM OFDM signal, when the gain of the PGA was 69 dB and the transmission distance was 20 m.

made by the PGA. The remaining capacity of the two batteries is shown in the upper-right corner of the display screen. It is clear that the gain of the PGA gradually decreased from 73 dB to 69 dB with the consumption of electricity. As illustrated in Fig. 7, when the gain of the PGA decreased from 73 dB to 69 dB, the BERs of the 1.2-Mbit/s 4-QAM OFDM signal fluctuated within a small range (on the order of 10^{-4}), but were all below the FEC limit. The inset is a constellation map of the 1.2-Mbit/s 4-QAM OFDM signal when the gain of the PGA was 69 dB, which converged well. This means that even though the gain of the PGA decreased to 69 dB as the battery level dropped, it was still high enough to provide a high SNR and, thus, support 1.2-Mbit/s data transmission over 20 m.

3. Field Trial on a Solar Cell Testbed

3.1 Experimental Setup

Fig. 8(a) shows the experimental scene of the AquaE-lite and white-light laser-based VLC in an outdoor PV solar cell testbed located at KAUST (39°06' E, 22°17' N). The white-light laser and AquaE-lite are shown in Figs. 8(b) and 8(c), respectively.

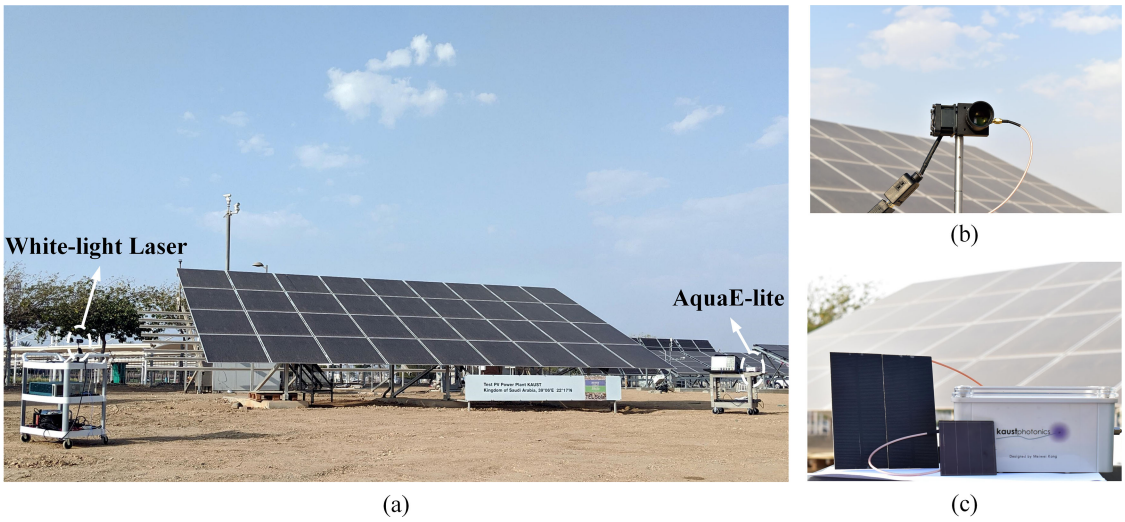

Fig. 8. (a) Experimental scene of the AquaE-lite and white-light laser-based VLC system on a PV solar cell testbed, the New Energy Oasis site, at KAUST (39°06' E, 22°17' N), (b) white-light laser, and (c) AquaE-lite.

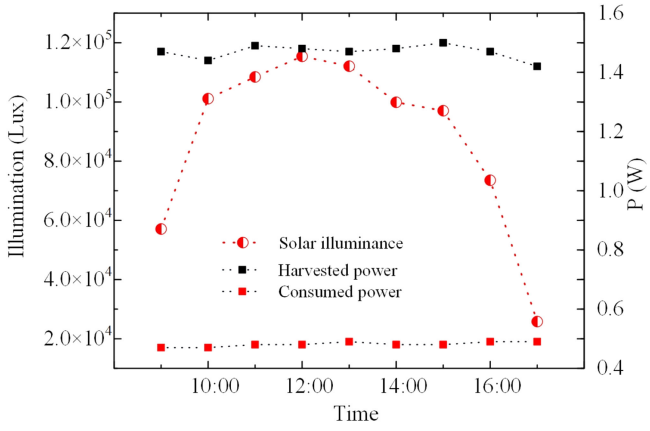

Fig. 9. Measured solar illuminance, power harvested by the monocrystalline Si solar panel, and power consumed by the receiver circuit of AquaE-lite at different time on the PV solar cell testbed located at KAUST (39°06' E, 22°17' N).

3.2 Experimental Results

In the field trial, we first measured the solar illuminance, the power harvested by the monocrystalline Si solar panel, and the power consumed by the receiver circuit of AquaE-lite at different times as shown in Fig. 9. The solar illuminance increased from 9:00 to 12:00 and decreased from 12:00 to 17:00. Both the harvested and the consumed power fluctuated in a narrow range at different times, but the overall power harvested was always greater than the power consumed. This indicates that AquaE-lite was energy autonomous. The extra harvested energy was stored in the battery for backup. In future applications, the harvested power can be further increased by using an autonomous Sun-tracking system, and the consumed power can be further decreased by using wake-up strategies, where this is beneficial for shortening the charging time of the battery.

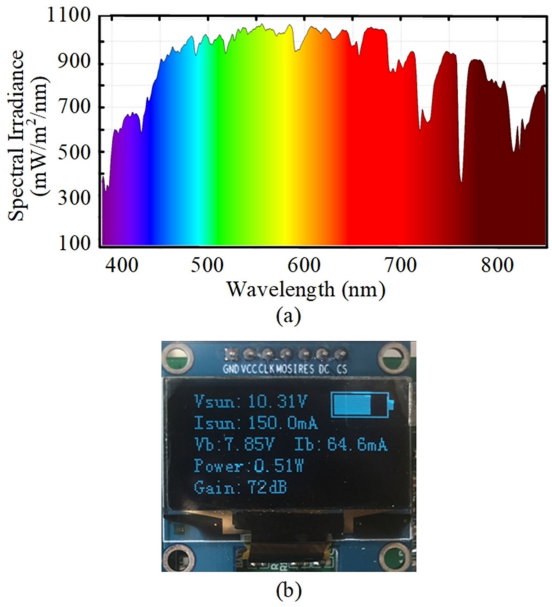

Fig. 10. (a) Solar spectrum measured during the field trial on the solar cell testbed located at KAUST (39°06' E, 22°17' N), and (b) photo of the display screen on the receiver circuit of AquaE-lite, where the output voltage (V_{sun}) and the current (I_{sun}) of the monocrystalline Si solar panel for energy harvesting were 10.31 V and 150.0 mA, respectively; the total consumed voltage (V_b) and current (I_b) of the two batteries on the receiver circuit of AquaE-lite were 7.85 V and 64.6 mA, respectively; the power consumed by the receiver circuit of AquaE-lite (Power) was 0.51 W; the PGA gain value (Gain) was 72 dB.

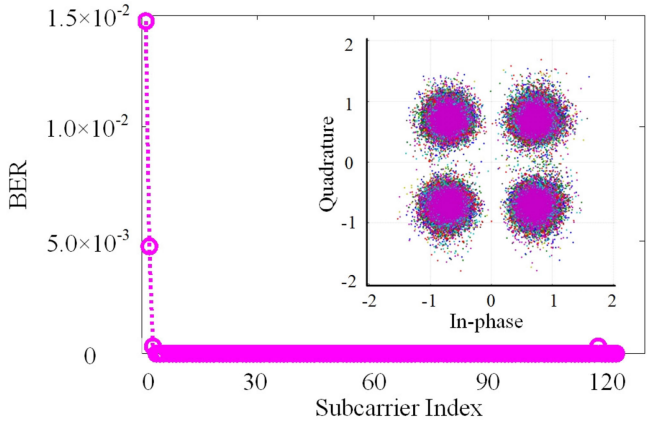

Fig. 11. BERs of the received 1.2-Mbit/s OFDM signals for different subcarriers after transmission through a 15-m air channel on the solar cell testbed located at KAUST (39°06' E, 22°17' N). Inset: the corresponding constellation map.

We then demonstrated the superiority of the white-light laser and AquaE-lite in implementing long-distance VLC under strong background sunlight. Fig. 10(a) illustrates the solar spectrum measured during the field trial. The illuminance of the sunlight was measured at 75080.28 lx. In bright sunlight, the recorded parameters of AquaE-lite for simultaneous energy harvesting and VLC are illustrated in Fig. 10(b). On the display screen, V_{sun} and I_{sun} were 10.31 V and 150 mA, respectively. Thus, the power harvested from sunlight was 1.5465 W. V_b and I_b were 7.85 V and 64.6 mA, respectively. Thus, the power consumed by AquaE-lite was 0.51 W. Under the given circumstances, the Gain was 72 dB, and 1.2-Mbit/s 4-QAM OFDM signals were obtained after transmitting through a 15-m air channel. Fig. 11 shows BERs of the received 1.2-Mbit/s OFDM

Fig. 12. (a) The KAUST harbor by the Red Sea, (b) the experimental scene of the AquaE-lite and white-light laser-based VLC system, (c) the capsule of the transmitter, and (d) the receiver's capsule.

signals for different subcarriers. Higher BERs in the low-frequency regions were attributed to the strong optical background noise. However, the total BER was 1.624×10^{-4}, which was below the FEC limit. The corresponding constellation map is shown in the inset of Fig. 11, and converges well. This indicates that AquaE-lite has good performance in low-intensity optical signal detection and resistance to background noise over long-distance VLC under strong sunlight.

4. Field Trial at a Port

4.1 Experimental Setup

We further investigated the communication performance of AquaE-lite at the KAUST harbor as shown in Fig. 12(a). Fig. 12(b) shows the experimental scene of AquaE-lite and the white-light laser-based VLC system. Figs. 12(c) and 12(d) present the capsules of the transmitter and the receiver, where the white-light laser and the a-Si thin film solar cell were installed, respectively. The receiver circuit of AquaE-lite and the other devices (e.g., AWG, Bias-T, AMP, ATT, and MSO) on the transmitter and receiver sides were placed on the shore, as those shown in Fig. 1(b). Note that the transmitter and the receiver were not aligned well due to the uneven ground as shown in Fig. 12(a). Moreover, as the field trial in the harbor was primarily designed to test communication performance, the monocrystalline Si solar panel used for energy harvesting was not connected to AquaE-lite. In future work, AquaE-lite can be deployed on the surface of water or in shallow water, where sunlight can reach, to implement simultaneous energy harvesting and VLC. It can also be installed on autonomous underwater vehicles, which can hover over the surface of water or in shallow water to recharge after completing missions in deep water. Thus, it will play an important role in future self-powered Internet of Underwater Things to significantly alleviate underwater energy-shortage issues.

4.2 Experimental Results

Fig. 13 shows the absorption, scattering, and attenuation coefficients of the water, *a*, *b*, and *c*, respectively, measured by an ac-s Spectral Absorption and Attenuation Sensor at different wavelengths, λ. According to these values, the water type at the harbor was optically complex waters like coastal area where it is dominated by inorganic suspended particles such as sediments [17]. As shown in Figs. 12(c) and (d), a variety of suspended particles were suspended between the transmitter and the receiver. In these circumstances, 2-m transmission distance was still achieved at a data rate of 1.2 Mbit/s without strict link alignment. Fig. 14 shows BERs of the received

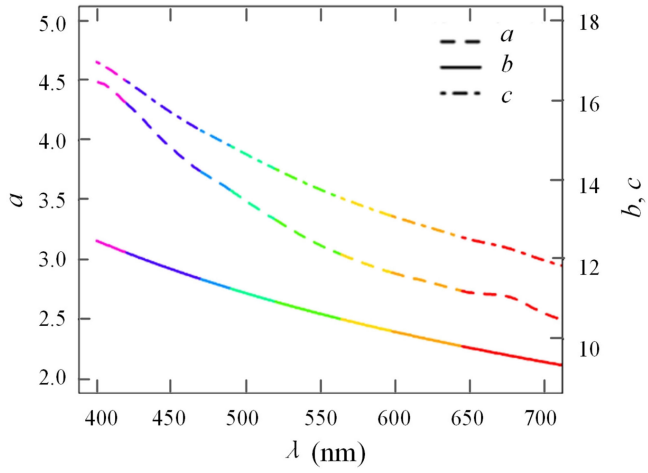

Fig. 13. Absorption, scattering, and attenuation coefficients of the water at the KAUST harbor by the Red Sea, *a*, *b*, and *c*, respectively, measured by an ac-s Spectral Absorption and Attenuation Sensor at different wavelengths, λ.

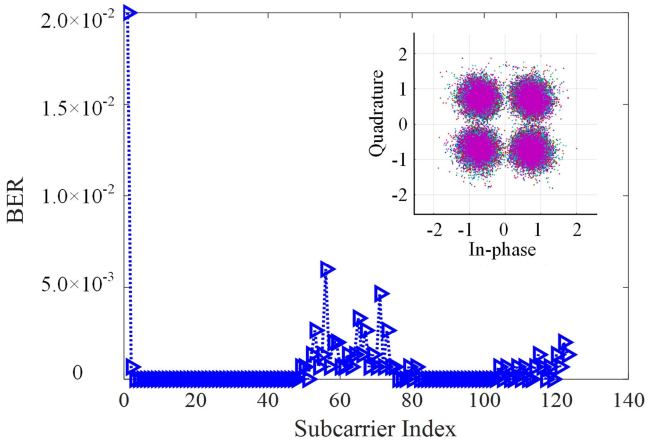

Fig. 14. BERs of the received 1.2-Mbit/s OFDM signals for different subcarriers after transmission through a 2-m turbid water channel. Inset: the corresponding constellation map.

1.2-Mbit/s OFDM signals for all subcarriers. Some random noise is evident in the spectrum. However, the mean BER was 6.125×10^{-4}, which was below the FEC limit. The corresponding constellation map is shown in the inset of Fig. 14, which converged well. This indicates that AquaE-lite with the advantages of large detection area, supporting low-intensity optical signal detection, and resistance to background noise has good robustness in the turbid water. Moreover, given these advantages, AquaE-lite has great potential in future underwater mobile sensor networks to relieve the strict requirements for pointing, acquisition and tracking.

5. Conclusion

In this work, a prototype called AquaE-lite hybrid-solar-cell receiver-modality, consisting of two kinds of solar cells for simultaneous efficient energy harvesting and low-intensity optical signal detection, has been developed and demonstrated. The results obtained on the laboratory testbed and various field trials are listed in Table 1. Using hardware pre-equalization technology, the -3-dB bandwidth of AquaE-lite was improved from 290 kHz to 340 kHz and the achievable data rate at

TABLE 1
Results Obtained on the Laboratory Testbed and in Various Field Trials

	Laboratory testbed		Outdoor solar cell testbed	Harbor (turbid water)
Data rate (Mbit/s)	1.6	1.2	1.2	1.2
Transmission distance (m)	20	30	15	2
BER	1.814×10^{-3}	2.131×10^{-3}	1.624×10^{-4}	6.125×10^{-4}

a distance of 20 m was improved from 1 Mbit/s to 1.6 Mbit/s by using OFDM on the laboratory testbed. Moreover, a 30-m long-distance illumination and VLC were implemented at a data rate of 1.2 Mbit/s due to the high absorption efficient of the thin-film a-Si solar cell. On the outdoor solar cell testbed, AquaE-lite delivered good performance in terms of resistance to background noise, which was attributed to the PGA and filter design in the hardware, gap design in OFDM, and selection of low-noise components. Under bright sunlight, energy autonomy was realized and a 15-m transmission distance was achieved at a data rate of 1.2 Mbit/s. In a more challenging field trial conducted at the KAUST harbor located by the Red Sea, 1.2-Mbit/s OFDM signals were obtained over a 2-m transmission distance without strict link alignment, which demonstrated the good robustness of AquaE-lite with a large detection area. Given the above, energy-autonomous solar cell receivers with the advantages of efficient energy harvesting, low-intensity optical signal detection, and resistance to background noise have broad application prospects in future IoT and underwater mobile sensor networks. Future work will involve replacing the MSO and off-line processing with a real-time digital signal processing module to implement fully energy-autonomous solar-cell receivers.

Acknowledgment

The authors further acknowledge the access of the New Energy Oasis (NEO) outdoor testing facilities at KAUST and the KAUST harbor.

References

[1] W. Su and A. Q. Huang, *The Energy Internet: An Open Energy Platform to Transform Legacy Power Systems into Open Innovation and Global Economic Engines*. Woodhead Publishing, 2018.
[2] W. A. Badawy, "A review on solar cells from Si-single crystals to porous materials and quantum dots," *J. Adv. Res.*, vol. 6, no. 2, pp. 123–132, 2015.
[3] M. Nayfeh, "Advanced and low cost energy and lighting devices," *Fundam. Appl. Nano Silicon Plasmonics Fullerines*, vol. 2018, pp. 363–429, Jan. 2018.
[4] Oxford PV. Oxford PV perovskite solar cell achieves 28% efficiency, 2018. [Online]. Available: https://www.oxfordpv.com/news/oxford-pv-perovskite-solar-cell-achieves-28-efficiency. Accessed on: Apr. 16, 2019
[5] M. Kong *et al.*, "Toward self-powered and reliable visible light communication using amorphous silicon thin-film solar cells," *Opt. Express*, vol. 27, pp. 34542–34551, 2019.
[6] J. Fakidis, S. Videv, H. Helmers, and H. Haas, "0.5-Gb/s OFDM-based laser data and power transfer using a GaAs photovoltaic cell," *IEEE Photon. Technol. Lett.*, vol. 30, no. 9, pp. 841–844, May 2018.
[7] M. Kong *et al.*, "Underwater wireless optical communication using a lens-free solar panel receiver," *Opt. Commun.*, vol. 426, pp. 94–98, 2018.
[8] H. Y. Wang *et al.*, "Using pre-distorted PAM-4 signal and parallel resistance circuit to enhance the passive solar cell based visible light communication," *Opt. Commun.*, vol. 407, pp. 245–249, 2018.
[9] X. Chen, C. Min, and J. Guo, "Visible light communication system using silicon photocell for energy gathering and data receiving," *Int. J. Opt.*, vol. 2017, pp. 1–5, 2017.
[10] W. H. Shin, S. H. Yang, D. H. Kwon, and S. K. Han, "Self-reverse-biased solar panel optical receiver for simultaneous visible light communication and energy harvesting," *Opt. Express*, vol. 24, no. 22, pp. A1300–A1305, 2016.
[11] S. M. Kim, J. S. Won, and S. H. Nahm, "Simultaneous reception of solar power and visible light communication using a solar cell," *Opt. Eng.*, vol. 53, no. 4, 2014, Art. no. 046103.
[12] J. I. de Oliveira Filho, A. Trichili, B. S. Ooi, M. S. Alouini, and K. N. Salama, "Toward self-powered Internet of Underwater Things devices," *IEEE Commun. Mag.*, vol. 58, no. 1, pp. 68–73, Jan. 2020.

[13] P. Pešek *et al.*, "Mobile user connectivity in relay-assisted visible light communications," *Sensors*, vol. 18, no. 4, 2018, Art. no. 1125.
[14] P. Saxena and M. R. Bhatnagar, "A simplified form of beam spread function in underwater wireless optical communication and its applications," *IEEE Access*, vol. 7, pp. 105298–105313, 2019.
[15] Mobile IoT in the 5G future. GSMA. 2020. [Online]. Available: https://www.ericsson.com/4a8d35/assets/local/networks/documents/gsma-5g-mobile-iot.pdf
[16] A. Froytlog *et al.*, "Ultra-low power wake-up radio for 5G IoT," *IEEE Commun. Mag.*, vol. 57, no. 3, pp. 111–117, Mar. 2019.
[17] A. Morel, and L. Prieur, "Analysis of variations in ocean color 1," *Limnology Oceanogr.*, vol. 22, no. 4, pp. 709–722, 1977.